

Figure 1. Systematic approach for obtaining tissue-of-action scores. Fine-mapping of conditionally-independent GWAS signals results in a set of credible variants, each with a posterior probability of association (PPA). The illustrated example shows a signal with five SNPs in its credible set with SNP₃ as the variant with the maximum PPA. Each credible SNP is then mapped to a panel of chromatin state annotations across four disease-relevant tissues to obtain a set of annotation vectors (**Step 1A**). An additional annotation vector for SNPs mapping to coding sequence (CDS) is obtained from expression specificity scores (ESS) calculated from gene expression levels across the four tissues (**Step 1B**). The set of annotation vectors for each SNP are then summed and scaled, yielding a vector used to partition the PPA value (**Step 2**). The resultant vectors for each SNP in a genetic credible set are then summed and scaled to yield a tissue-of-action (TOA) score for each tissue at the GWAS signal corresponding to the credible set (**Step 3**). Any residual PPA values from SNPs not mapping to any of the evaluated tissue annotations are allocated to an “unclassified” score (grey column in matrix).

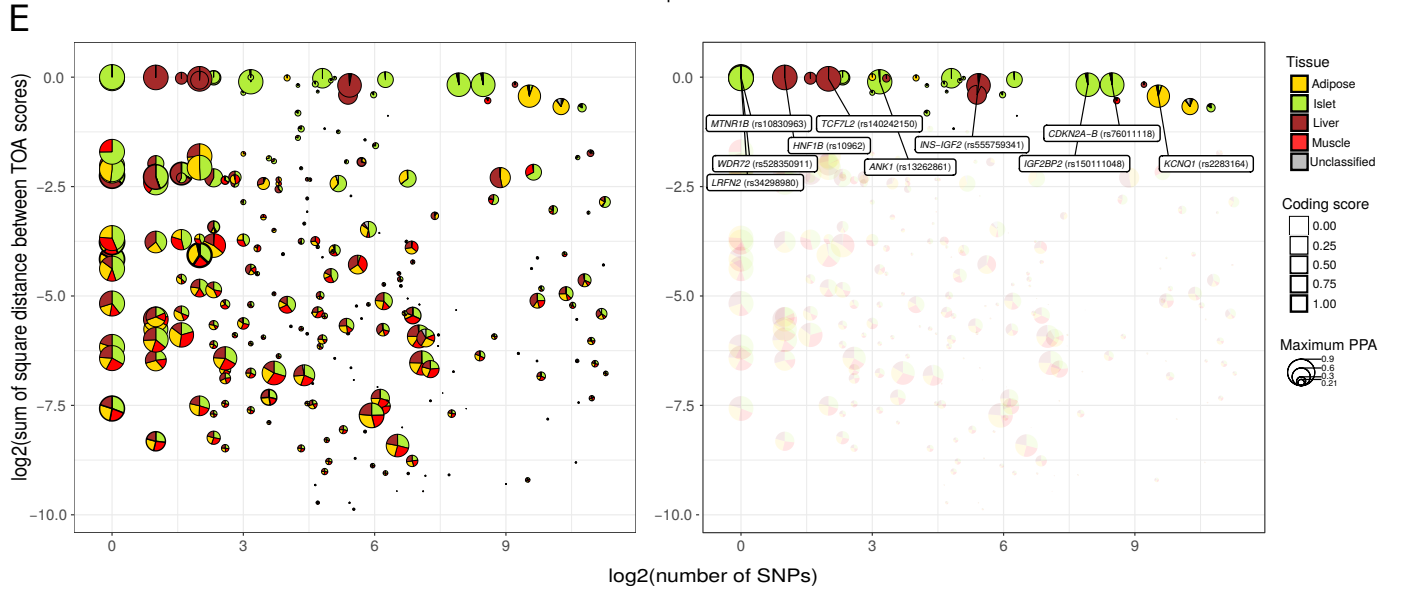
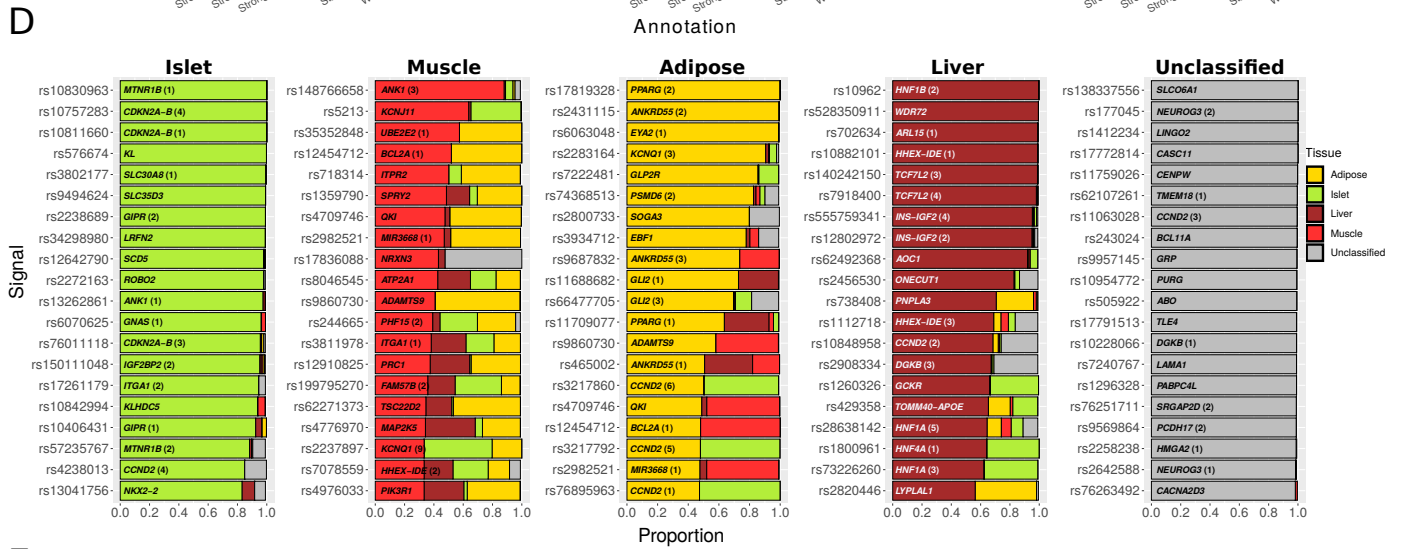
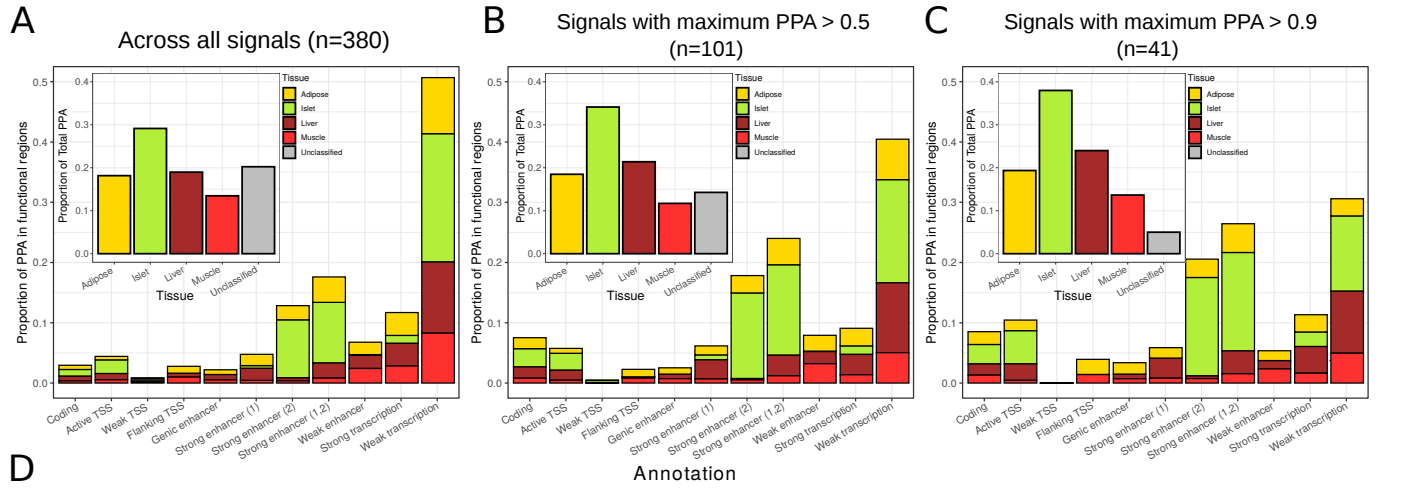


Figure 2. The profile of tissue-of-action scores across T2D signals. **A)** The proportion of total PPA summed across all 380 signals is shown for each tissue (inset). The proportion of total PPA is also shown for each annotation group (outset). Proportions are also exhibited for the subset of signals with maximum credible set PPA > 0.5 in panel **B** and for the subset of signals with maximum PPA > 0.9 in panel **C**. **D)** The profile of TOA scores is shown for the top 20 signals ranked for each tissue. The locus name and rs accession number for the index SNP is indicated for each signal. Signals at loci with multiple conditionally-independent signals are indicated by parenthetical numbers (i.e. one is primary signal, two is secondary signal, etc.). **E)** Relationship between fine-mapping resolution and TOA score diversity. Log₂ of the number of credible SNPs for each fine-mapped signal is shown on the x-axis and the log₂ value of the sum of square differences between TOA scores for each signal is shown on the y-axis (i.e. higher values on the y-axis correspond to greater tissue “specificity”). The profile of TOA scores are indicated within pie charts where the diameter of each circle corresponds to the maximum PPA for the credible set. The line thickness for each circle indicates a coding score for each credible set (i.e. the proportion of cumulative PPA attributable to coding variants). The left panel shows all credible sets with unclassified scores < 0.10 (n=259) and the right panel highlights the subset of “tissue-specific” signals with TOA scores ≥ 0.8 . The ten “tissue-specific” signals with the highest maximum credible set PPA are labeled in the right panel.

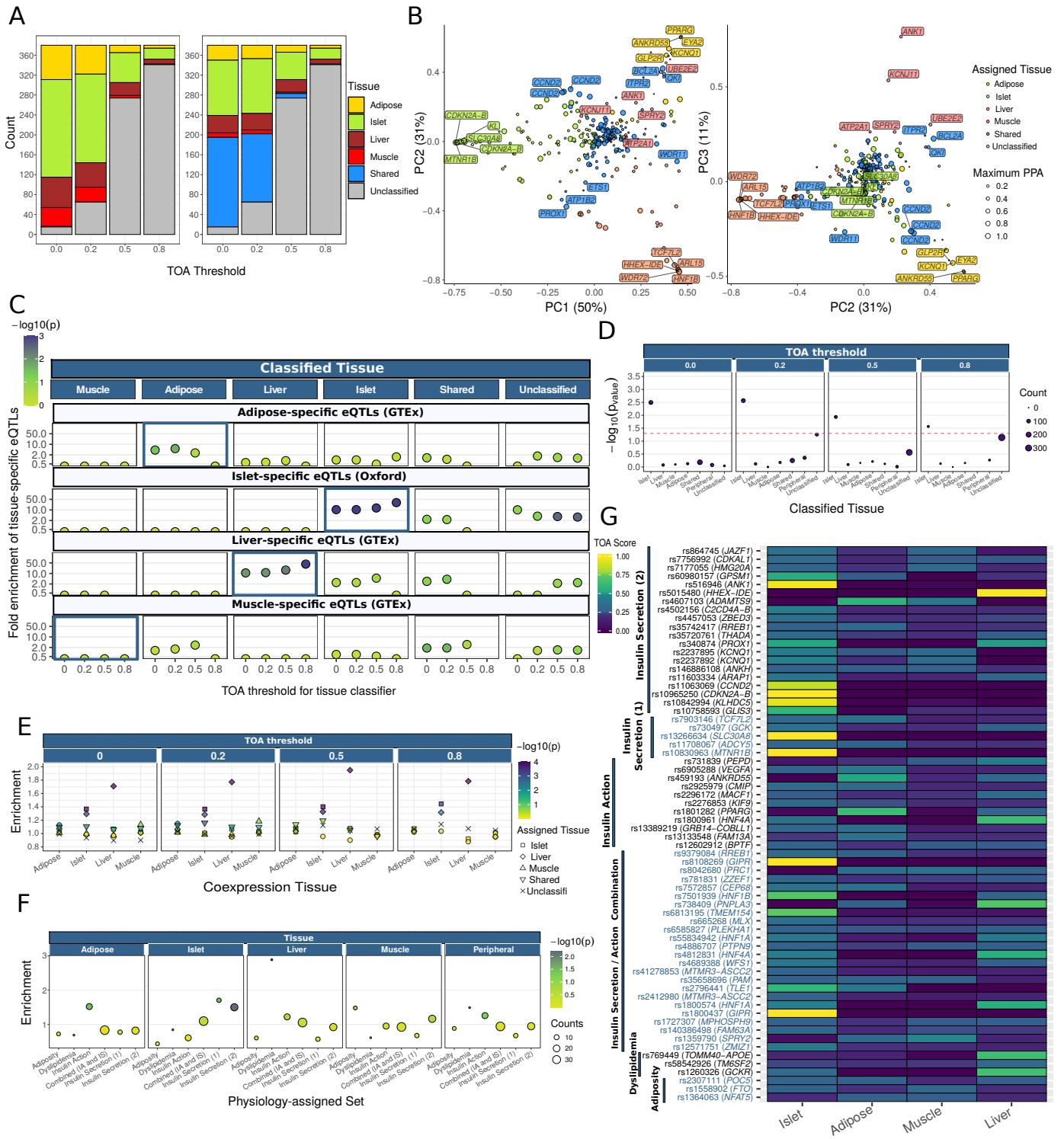


Figure 3. Enrichment of tissue-specific epigenomic and physiological features among classified signals. **A)** Number of signals assigned to each tissue by the classifier for each of the four TOA score thresholds: 0.0, 0.2, 0.5, and 0.8 (left panel). Signal counts are shown across thresholds using a classifier that assigns signals with two or more TOA scores within 0.1 of each other as “shared” signals (right panel). **B)** PCA plots of the decomposition of the TOA score matrix comprising the 306 signals with “unclassified” scores ≤ 0.5 . Each point corresponds to a signal where the size indicates the maximum credible set PPA and the color indicates the assigned tissue at the TOA score threshold ≥ 0.2 using the classifier that included a “shared” designation. **C)** Selective enrichment of tissue-specific eQTLs among credible sets for signals assigned to subcutaneous adipose, islet, liver, and skeletal muscle tissue. Color indicates significance of enrichment. **D)** Selective improvement in fine-mapping resolution at islet-assigned signals when richer islet chromatin states are deployed. Comparison of *functional* fine-mapping resolution using a panel of chromatin state annotations based on histone ChIP-seq across the four T2D relevant tissues versus chromatin states based on islet ChIP-seq, ATAC-seq, and DNA methylation (WGBS). **E)** Coexpression of nearest genes annotated to sets of tissue-assigned signals across stringency thresholds. Shape indicates the tissue to which the set of signals were assigned. **F)** Selective TOA score enrichment within relevant sets of physiology-assigned signals. Size corresponds to the number assigned signals in each physiology group. **G)** Tile plot of TOA scores for physiologically-assigned signals. Signals are ordered by physiology group and the corresponding GWAS locus is shown.

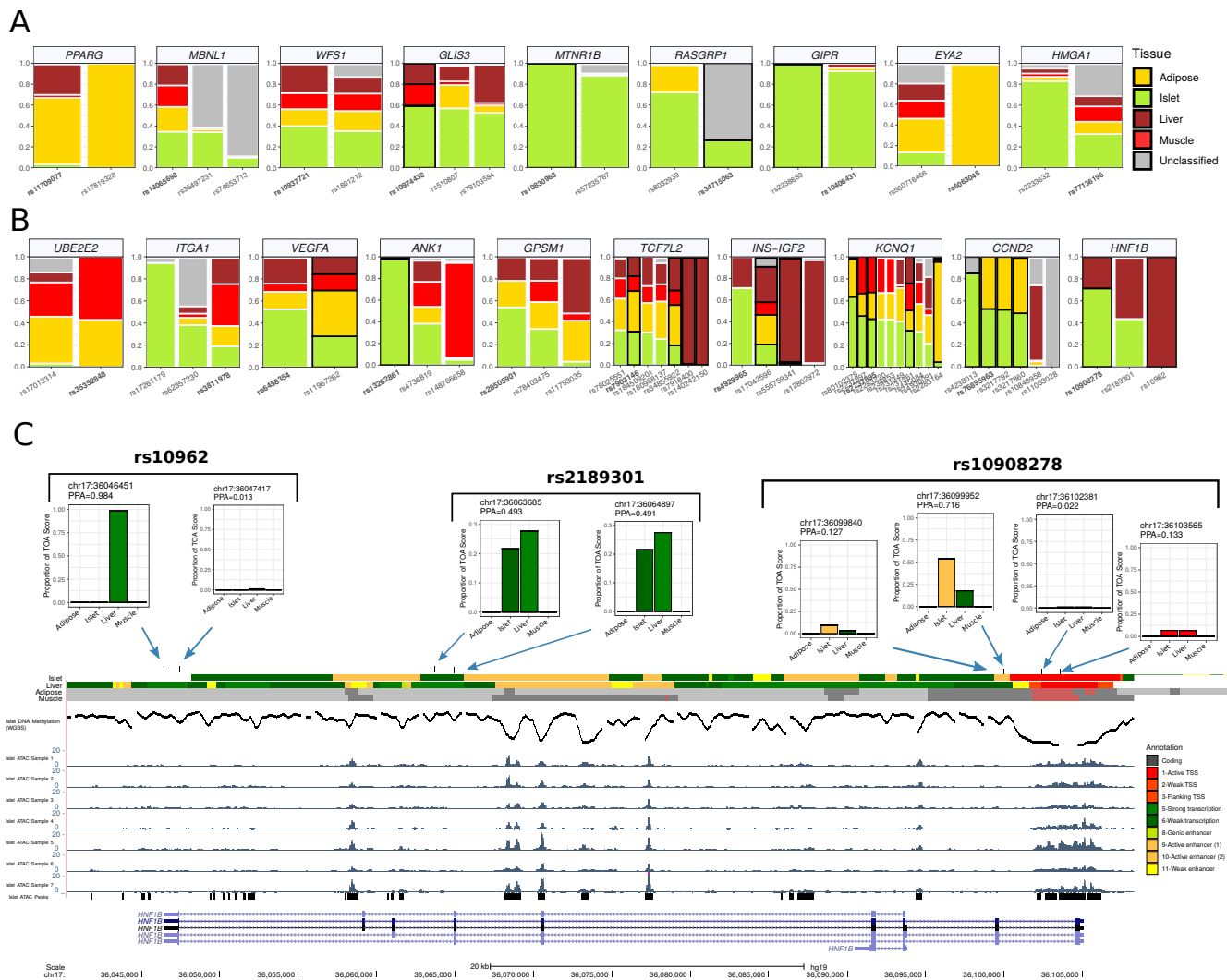


Figure 4. Multiple tissues implicated by epigenomic scores at heterogenous loci. A) Profile of TOA scores for the nine loci with all signals receiving identical, “non-shared” tissue assignments at the 0.2 stringency threshold B) Profile of TOA scores for the ten loci with all signals receiving distinct, “non-shared” tissue assignments at the 0.2 threshold. C) epigenomic profile of PPA values attributable to each credible SNP of the primary signal at the *HNF1B* locus. For each credible SNP, the PPA value attributable to each tissue annotation is shown along with its position on chromosome 17 (genome build hg19). Chromatin state maps for islet, adipose, muscle, and liver tissue from Varshney et al. 2017. are shown along with ATAC-seq tracks for seven representative islet samples, called ATAC-seq peaks from a set of islet ATAC samples (n=17), and DNA methylation (whole genome bisulfite sequencing) in human islets from Thurner et al. 2018.